Supporting Information

Pyrophosphate interlayer improves performance of semi-transparent perovskite solar cells

Jason J. Yoo,[†a] Jin-Won Lee,[†a] Yeonkyeong Ju,[a] Bong Joo Kang,[a] Youngwoong Kim,[a] Beom-Soo Kim,[a] Young Yun Kim,[a] Seong Sik Shin,[*a,c] Tae Joo Shin,[*b] Nam Joong Jeon[*a]

[a]Division of Advanced Materials, Korea Research Institute of Chemical Technology, 141 Gajeong-Ro, Yuseong-Gu, Daejeon 34114, Republic of Korea

[b]UNIST Central Research Facilities, Ulsan National Institute of Science and Technology (UNIST), 50 UNIST-gil, Ulsan, Korea

[c]SKKU Advanced Institute of Nanotechnology (SAINT) and Department of Nanoengineering, Sungkyunkwan University, Suwon 16419, Republic of Korea

†These authors contributed equally.

[*]Correspondence author. Email: njjeon@krict.re.kr (N.J.J.), tjshin@unist.ac.kr(T.J.S), sss85@skku.edu (S.S.S)

Average visible transmission (AVT) calculation

AVT is calculated by using the method reported by Yang et al.[1] The equation for calculating AVT is shown as following:

$$AVT = \frac{\int T(\lambda) \times AM1.5G(\lambda) \times P(\lambda) d\lambda}{\int AM1.5G(\lambda) \times P(\lambda) d\lambda}$$

where T(λ) is the transmission of the device, AM1.5G(λ) is the AM 1.5G spectrum, and P(λ) is human's photopic response.

Supplementary Figures

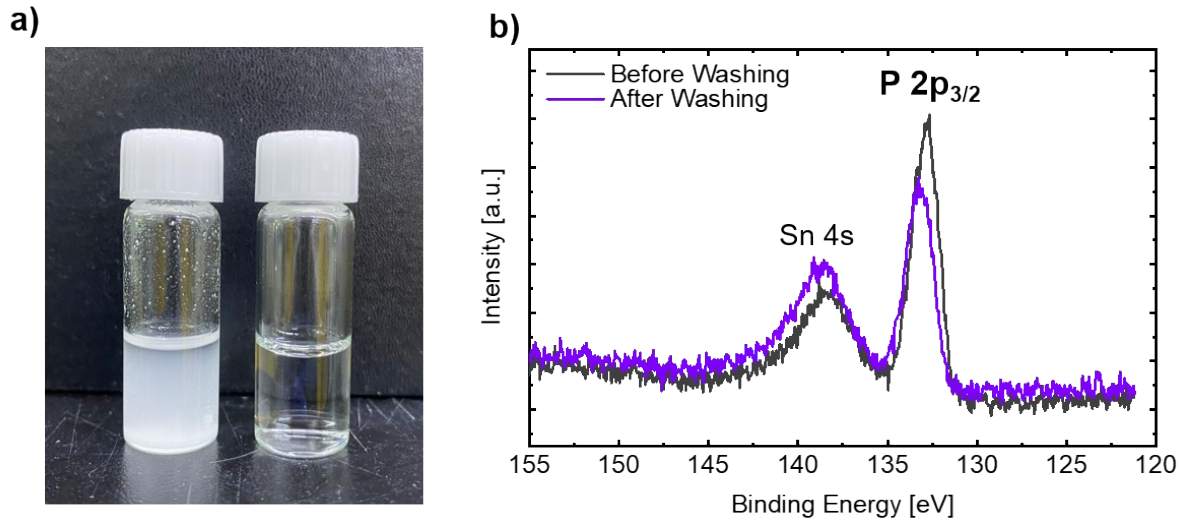

Figure S1

a) Photograph of KPP in DMF/DMSO solvent mixture (left) and in DI H_2O (right). This is to show the solute is not soluble in perovskite processing solvents (DMF/DMSO), hence will not be washed away during perovskite film deposition.

b) XPS spectra of SnO_2/KPP film before and after DMF/DMSO solvent washing. Majority of the peak intensity that correspond to P $2p_{3/2}$ is retained after solvent washing, suggesting KPP will not get washed away during perovskite film deposition.

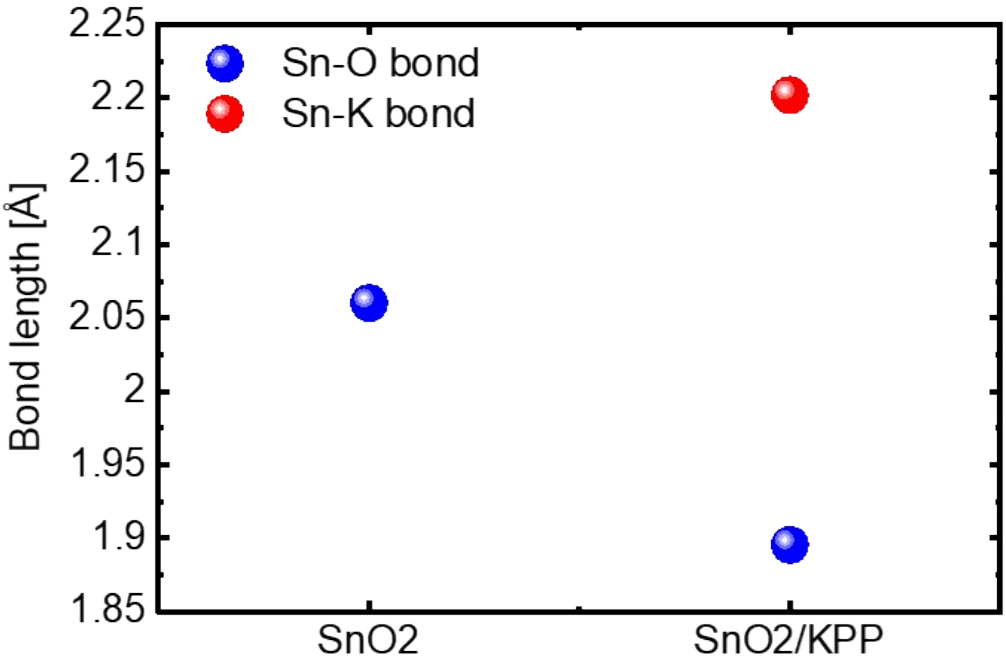

Figure S2

Sn-O and Sn-K bond length for the SnO_2 and SnO_2/KPP thin film. The data is extracted from the EXAFS results in Figure 1C. SnO_2/KPP sample shows shorter bond length for Sn-O, and shows presence of additional Sn-K bond of around 2.2 Å.

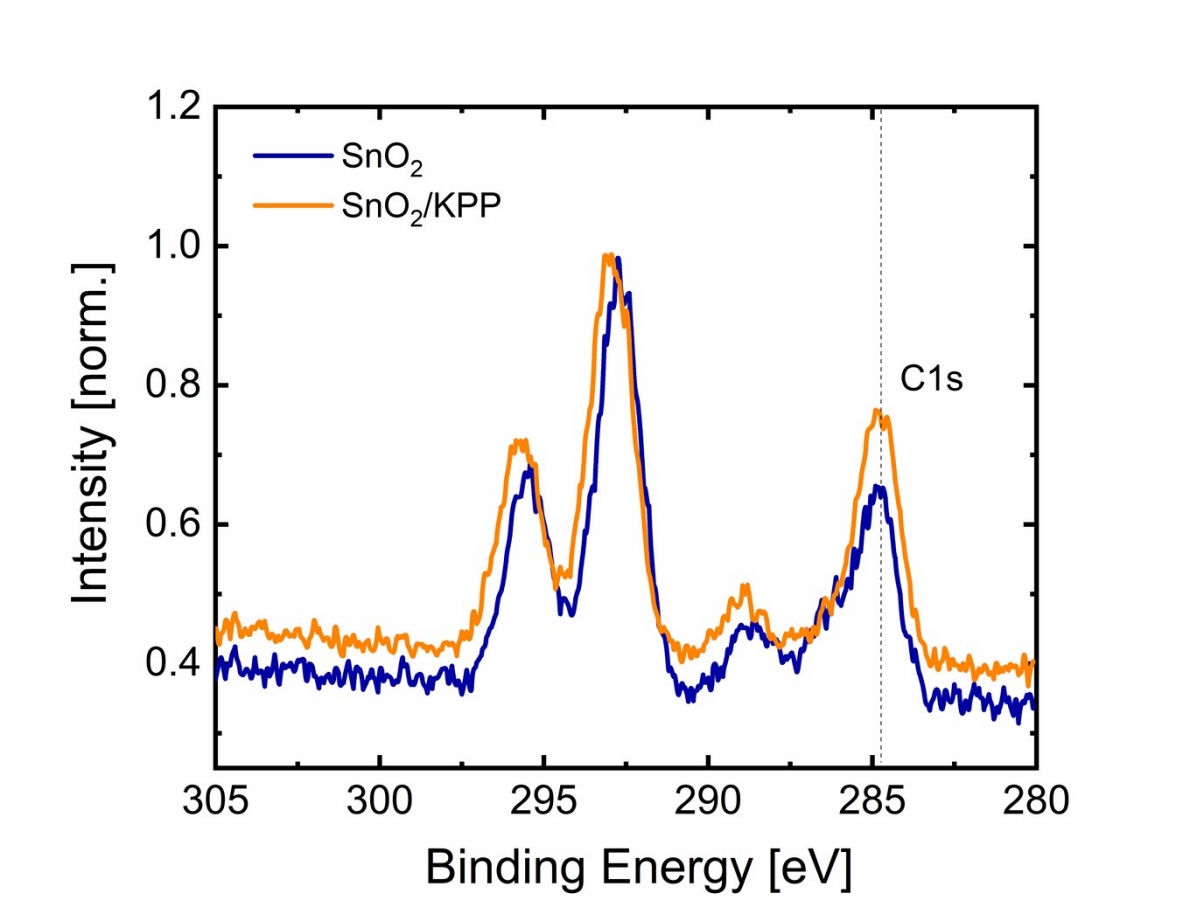

Figure S3

The binding energies in figure 1(d) have been calibrated by taking the carbon 1s peak as reference.

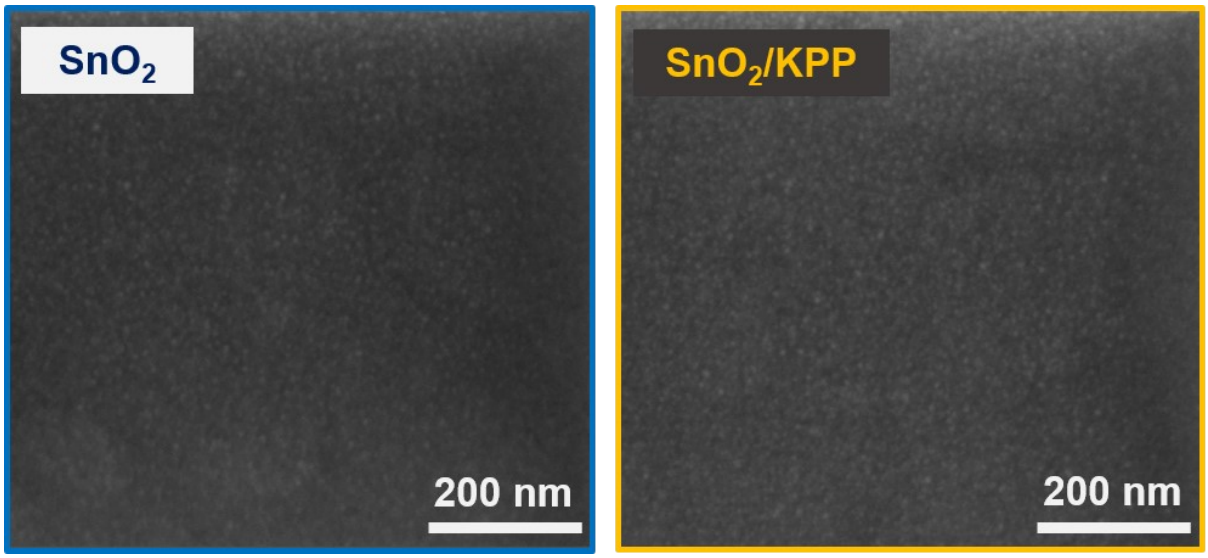

Figure S4

Surface SEM image of the SnO_2 and SnO_2/KPP thin film. No major change is observed upon deposition of the KPP interlayer.

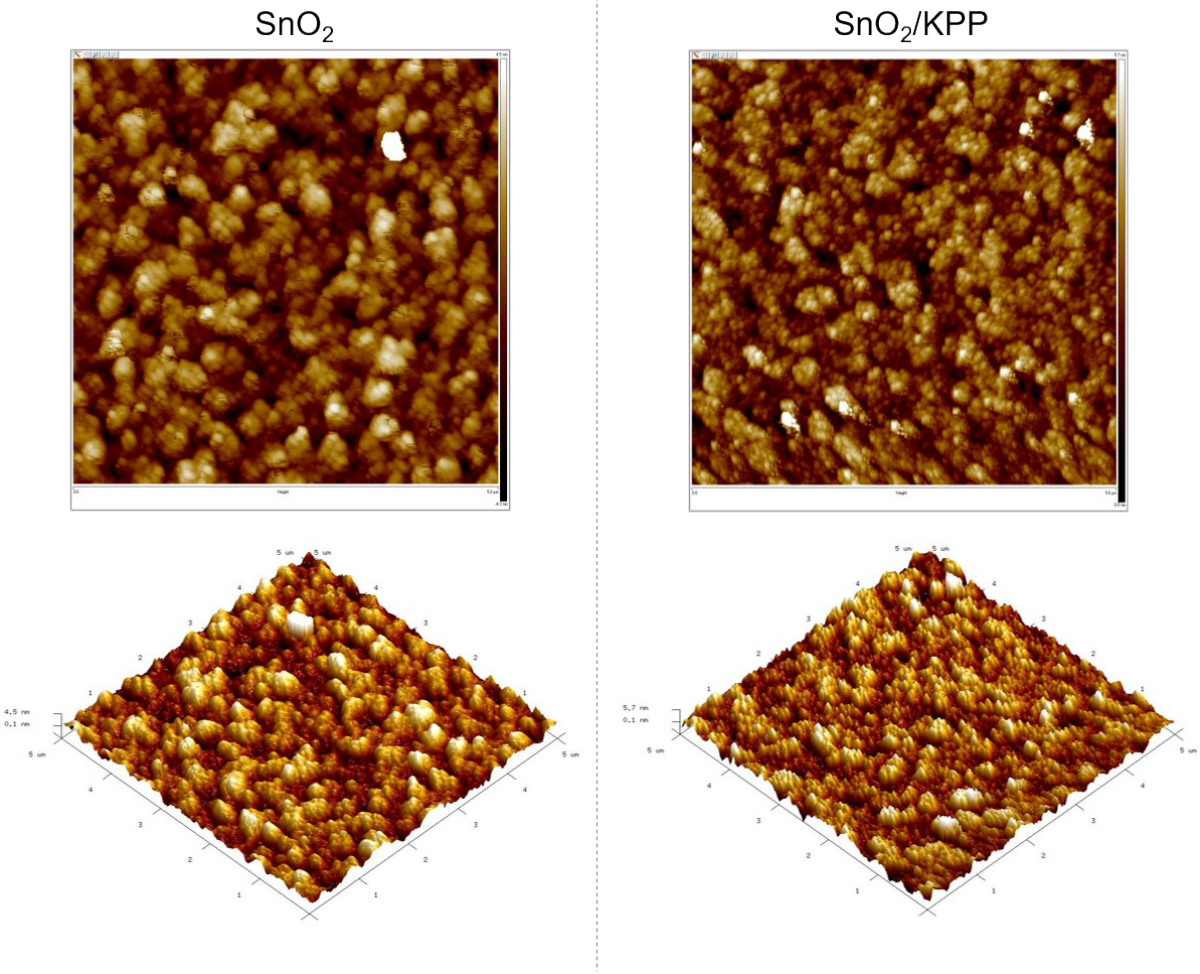

Figure S5

AFM images for the SnO_2 (left) and SnO_2/KPP (right) thin films.

Table S1. Crystallographic information abstained from XRD data in Figure 2d.

	Diffraction plane	2θ	[1]FWHM (°)	*d*-spacing (Å)	[2]L_c (nm)
SnO_2/perovskite	**$(100)_{cubic}$**	**13.930**	**0.146**	**6.352**	**57.03**
SnO_2/KPP/perovskite	**$(100)_{cubic}$**	**13.932**	**0.112**	**6.351**	**74.81**

[1]Full-width at half maximum

[2]Apparent crystallite size calculated from Scherrer equation

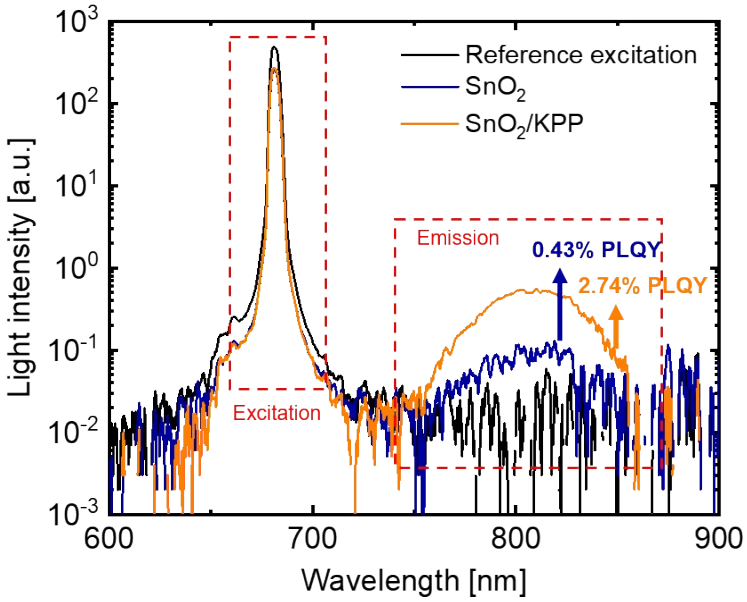

Figure S6

Spectra for the calculation of the photoluminescence quantum yield of the perovskite samples and with a KPP inter layer

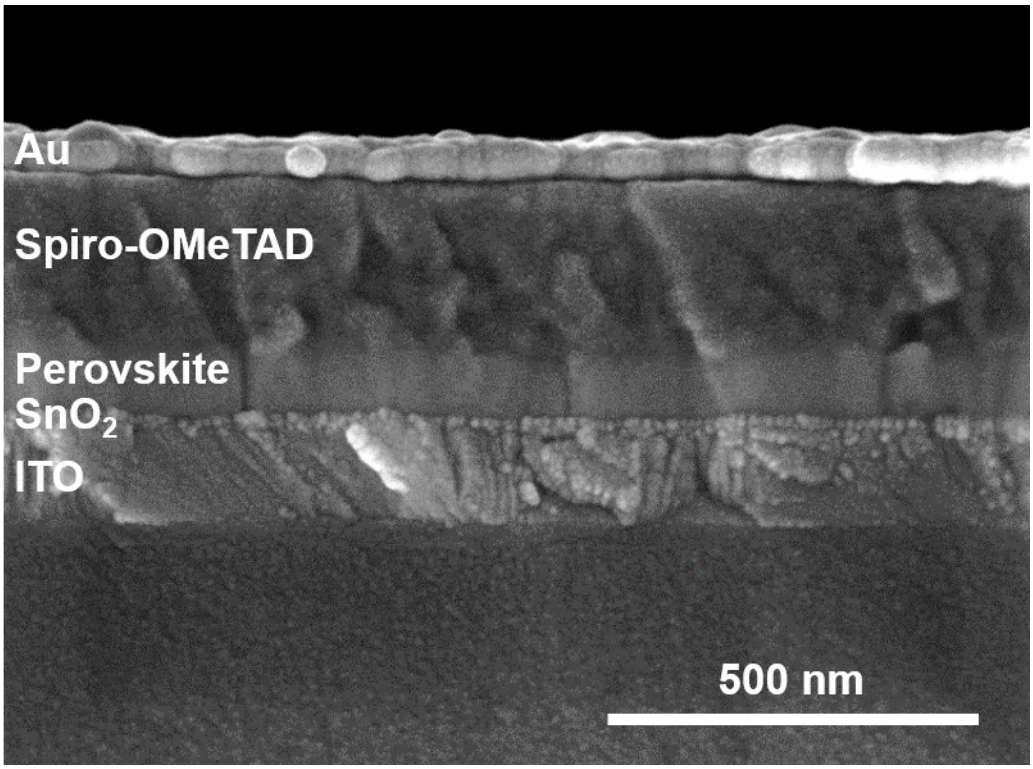

Figure S7

Cross-section SEM image of the opaque device with Spiro-OMeTAD and Au as the hole transporting layer and metal contact.

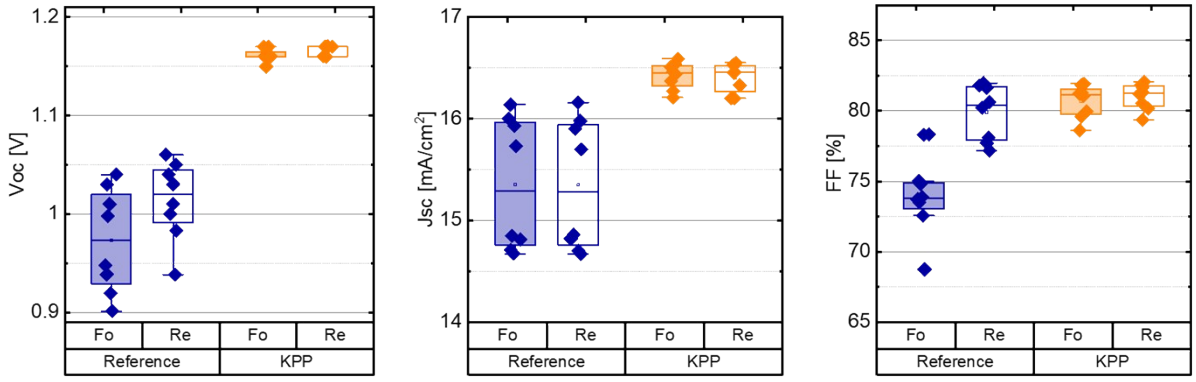

Figure S8

Statistical distribution for the Reference and KPP device for each device parameters. Data for PCE is shown in Figure 3b.

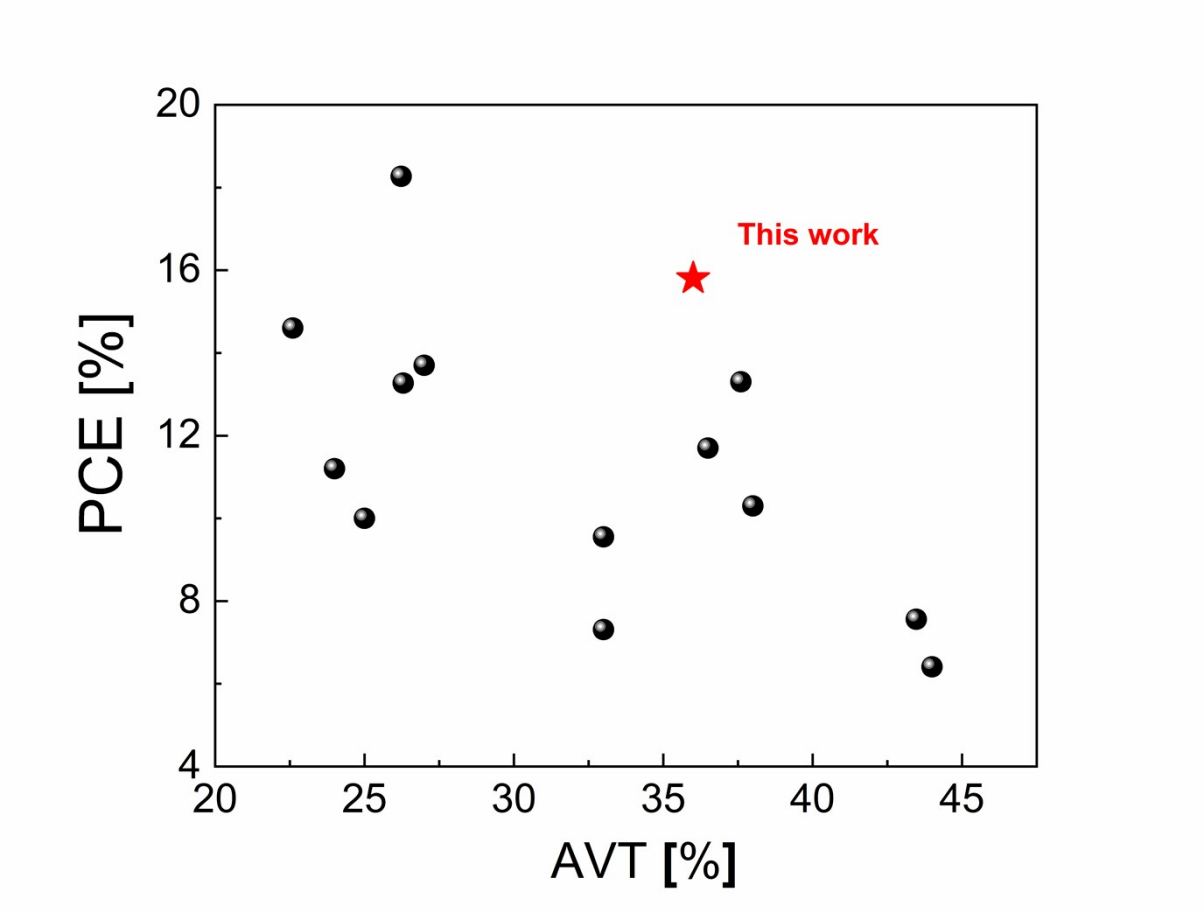

Figure S9

Plot of AVT vs PCE for semi-transparent perovskite solar cells. Our devices with KPP interlayer maintained high PCE at high AVT of ~36%.

Table S2. Literature summary on the AVT of semi-transparent perovskite solar cells without top electrodes and its PCE with opaque electrode.

Structure	AVT (%)	η (%)	Year	Ref.
ITO/PEDOT:PSS/polyTPD/Perovskite/PCBM	33	7.31	2014	[2]
ITO/PEDOT:PSS/polyTPD/Perovskite/PCBM	44	6.41	2014	[2]
ITO/CuSCN/Perovskite/PCBM	25	10	2015	[3]
ITO/PEDOT:PSS/Perovskite/PCBM	33	9.55	2015	[4]
FTO/c-TiO_2/AAO/Perovskite/Spiro	26.3	13.27	2016	[5]
FTO/c-TiO_2/Perovskite/Spiro	36.5	11.7	2016	[6]
FTO/c-TiO_2/Perovskite/Spiro	38	10.3	2017	[7]
FTO/c-TiO_2/Ink-TiO_2/Perovskite/Spiro	24	11.2	2021	[8]
FTO/SnO_2/Perovskite/Spiro	27	13.7	2022	[9]
FTO/SnO_2/Perovskite/Spiro	22.6	14.6	2023	[10]
FTO/c-TiO_2/Perovskite/PCBM	43.47	7.56	2023	[11]
FTO/c-TiO_2/Perovskite/Spiro	26.23	18.27	2023	[12]
FTO/c-TiO_2/Perovskite/Spiro	37.6	13.3	2023	[13]
ITO/KPP/SnO_2/Perovskite/Spiro	36	15.8	2024	This work

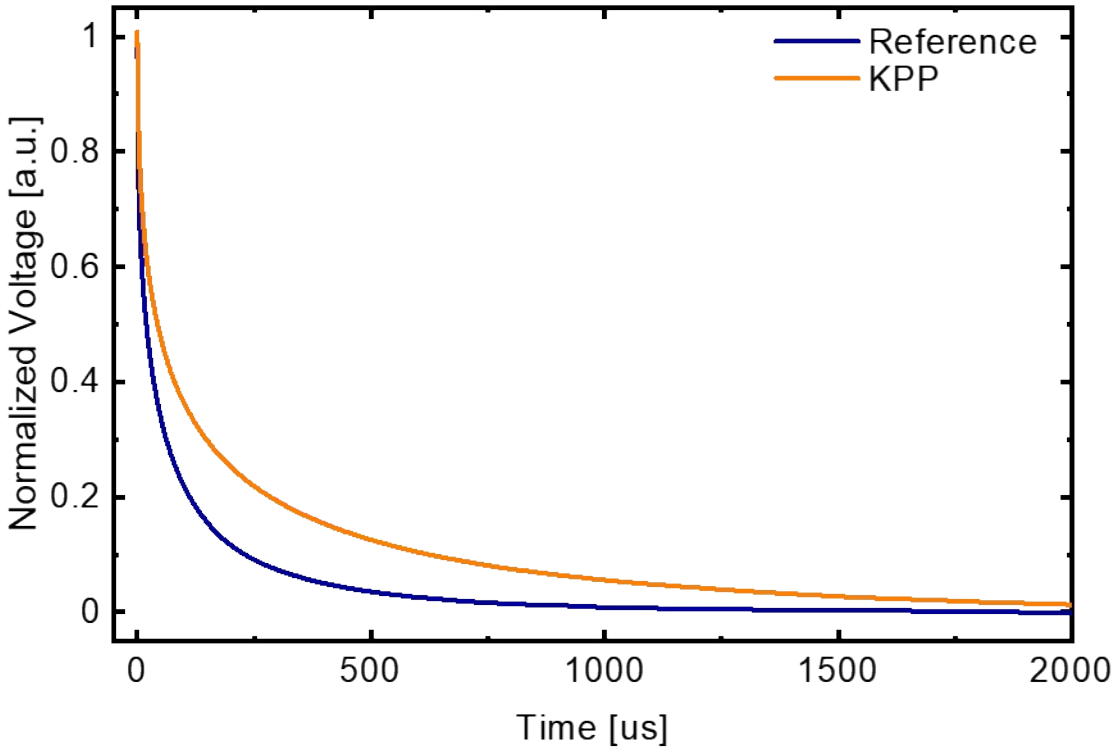

Figure S10

Transient photovoltage (TPV) decay curve for the Reference and KPP device. The KPP device exhibits longer decay lifetime (determined as the time it takes to each 1/e of initial) of 98 μs, when compared to that of Reference of 44 μs.

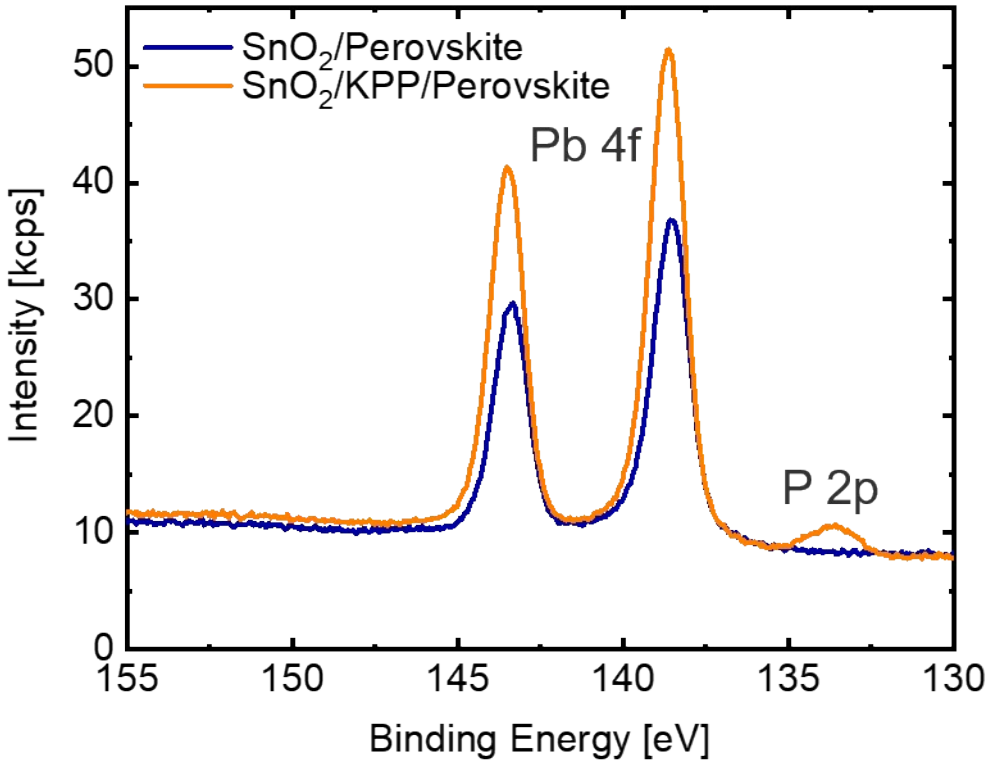

Figure S11

XPS spectra of SnO_2 surface after washing away the perovskite active layer with DMF/DMSO solvents. Higher signal for the KPP sample (orange trace) indicates stronger binding between the perovskite and its underlayer. In addition, the P 2P peak appears in the KPP-treated device differently from the reference device, indicating that the perovskite penetrates and interacts with the thin KPP layer. While shift of the Pb 4f binding energy towards lower energy for the Reference sample (blue trace) indicates formation of lead oxide derivatives, which can result in degradation of interface overtime.

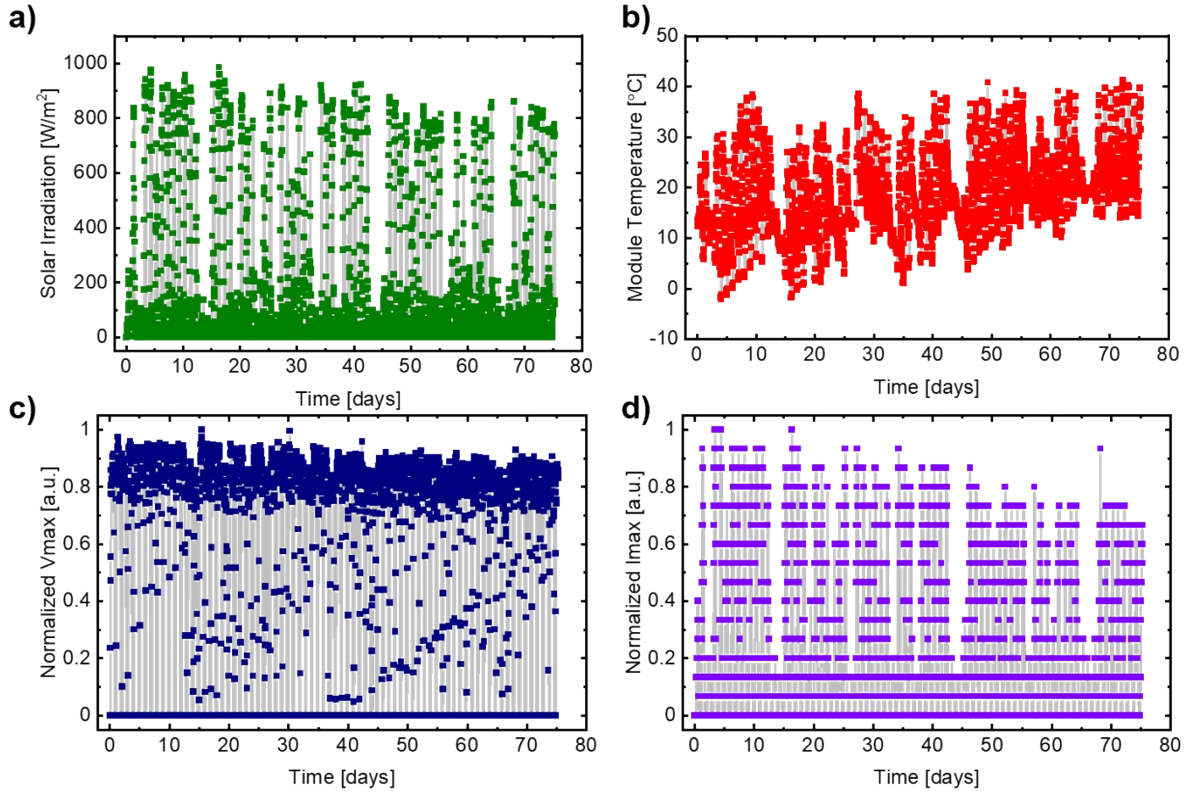

Figure S12

Plot of incident sunlight measured from a reference Si solar cell (a), the temperature of the semi-transparent module from the outdoor test setup (b), normalized maximum voltage (c) and maximum current (d).

References

1. J. Bing, L. G. Caro, H. P. Talathi, N. L. Chang, D. R. Mckenzie, A. W. Y. Ho-Baillie, *Joule.* 2022, **6**, 1446-1474.

2. C. Roldan-Carmona, O. Malinkiewicz, R. Betancur, G. Longo, C. Momblona, F. Jaramillo, L. Camacho, H. J. Bolink, *Energy Environ. Sci*. 2014, **7**, 2968-2973.

3. J. W. Jung, C. –C. Chueh, A. K. –Y. Jen, *Adv. Energy Mater*. 2015, **5**, 1500486.

4. C. O. R. Quiroz, I. Levchuk, C. Bronnbauer, M. Salvador, K. Forberich, T. Heumuller, Y. Hou, P. Schweizer, E. Spiecker, C. J. Brabec, *J. Mater. Chem. A* 2015, **3**, 24071-24081.

5. H. –C. Kwon, A. Kim, H. Lee, D. Lee, S. Jeong, J. Moon, *Adv. Energy Mater.* 2016, 1601055.

6. B. –X. Chen, H. –S. Rao, H. –Y. Chen, W. –G. Li, D. –B. Kuang, C. –Y. Su, *J. Mater. Chem. A* 2016, **4**, 15662-15669.

7. L. Zhang, M. T. Horantner, W. Zhang, Q. Yan, *Solar Energy Materials & Solar Cells* 2017, **160**, 193–202.

8. N. K. Pendyala, S. Magdassi, L. Etgar, *ACS Appl. Mater. Interfaces* 2021, **13**, 30524–30532.

9. S. Lie, A. Bruno, L. H. Wong, L. Etgar, *ACS Appl. Mater. Interfaces* 2022, **14**, 11339−11349.

10. A. Lorusso, S. Masi, C. Triolo, F. Mariano, S. Muia, A. Cannavale, Y. Duan, M. Anni, M. L. D. Giorgi, S. Patane, O. Selmi, I. Mora-Sero, S. D. Leo, M. Mazzeo, *Research square* 2023

11. J. Yang, Z. Wang, L. Liu, L. Wang, Z. Chang, J. Li, K. Wang, S. Liu, *Adv. Optical Mater.* 2023, **11**, 2203140.

12. Z. Yang, Y. Niu, X. Zhang, Z. Zhang, L. Hu, *Journal of Materials Chemistry A* 2023, **11**, 3070-3079.

13. J. Kim, D. Kim, W. Kim, S. Woo, S. -W. Baek, M. J. Ko, Y. Kim, *Chemical Engineering Journal* 2023, **469**, 143824.